U.S. DEPARTMENT OF COMMERCE
NATIONAL OCEANIC AND ATMOSPHERIC ADMINISTRATION
NATIONAL WEATHER SERVICE
NATIONAL METEOROLOGICAL CENTER

OFFICE NOTE 340

THE EFFECTS OF TURBULENT MIXING NEAR THE GROUND IN THE NESTED GRID MODEL

NORMAN A. PHILLIPS

APRIL 1988

The effects of turbulent mixing near the ground in the Nested Grid Model

N. Phillips

April 1988

A lecture prepared for the NMC internal training course on NWP physics and dynamics, April 1988

The fluxes of heat and moisture between land and atmosphere are calculated using formulas derived for the ECMWF by J.-F. Louis. Over land in the NGM, these formulas call for a large diurnal variation of the exchange coefficient, C.

upward turbulent flux of (momentum, heat, moisture) = (1)

C x density x wind speed x (wind speed, ground-air temperature difference, ground-air moisture difference)

Over water, the exchange coefficient in the NGM is based on the Charnock hypothesis that the roughness length z_o is appropriate for a saturated spectrum of the ocean waves, i.e., $z_o = g / u_*$ where u_* is the friction velocity. (Calculations of C were described in an earlier lecture by J. Tuccillo, and may be referred to in Tech. Proc. Bulletin 363.)

1. Vertical diffusion of momentum

A vertical diffusion of properties based on the austausch mechanism is used only for the horizontal velocity components u and v .

$$\frac{\partial u}{\partial t} = \text{other terms plus } \frac{1}{\rho}\frac{\partial}{\partial z}\left[\rho K \frac{\partial u}{\partial z}\right] . \qquad (2)$$

The present value for the austausch coefficient K used in the NGM is simply a constant (30 m^2/sec) divided by a term that is proportional to the local Richardson number:

$$K = \text{Austausch coefficient} = \frac{30\ (m^2/sec)}{1 + |Ri|} \qquad (3)$$

where

$$Ri = g\ \partial \ln \theta / \partial z \ / \ (\partial v / \partial z)^2 \qquad (4)$$

There is no experimental justification for the denominator of (3); it is intended merely to express the intuitive idea that there will be little vertical turbulent exchange when the atmosphere is stably stratified or when there is no vertical shear of the wind. The Richardson number is about 40 in the normal free atmosphere, but is zero when the temperature stratification is adiabatic. This gives K ≈ 1 m^2/sec in most of the atmosphere. This is a very small value and therefore friction has little direct effect on the prediction of velocities in the NGM away from the bottom layers. But the bottom layers can become adiabatically stratified during the day, so that K will then equal the large value of 30 m^2/sec, and create strong frictional effects in those layers.

The diurnal cycle will affect velocities over land in the bottom layers of the NGM through the diurnal variation of the surface exchange coefficient C (large in the day, small at night) and the diurnal variation of the austausch coefficient K . The resulting diurnal variation of wind speed in the bottom layer of the model over a region with moderate roughness length (z_o = 37 cms), high insolation and small moisture availability, is shown in Figure 1.

The speed is a maximum at night. This behavior is typical of the "nocturnal jet" that is common in the plains of the U.S., at elevations of 100 to 1000 meters. variables in the bottom layer of the NGM are about 150 meters above ground. Figure

2 is a reproduction of an analysis of observed data from this area by Bonner and Paegle (1970). The model evidently reproduces the observed diurnal behavior at this height.

Our more direct experience of diurnal winds is at anemometer height, which has a minimum speed at night. Test calculations have been made in which the vertical sigma layers in the NGM were changed so that the bottom-most level was only 50 meters above the ground. The diurnal behavior shown in Figure 1 was not changed. Test calculations have also been made in which the austausch coefficient increased with height (the von Karman "law of the wall", in which $K \propto z$). This also did not change the diurnal behavior in the bottom layer. It is believed that the prediction of a nocturnal minimum in speed in the bottom layer of the NGM will require very thin layers, and perhaps a formula for K that rapidly increases with height during the day and rapidly decreases with height during the night.

A wind at anemometer level can be defined by assuming that the stress $\rho\, C_d\, |\underset{\sim}{v}_1|^2$ that is computed in the model using the wind speed $|\underset{\sim}{v}_1|$ of layer one and the stability dependent drag coefficient C_d, can be matched to the stress from a hypothetical v_{an} at anemometer level:

$$\text{Stress} = \rho\, C_d\, |\underset{\sim}{v}_1|^2 = \rho\, C_N\, v_{an}^2 \qquad (5)$$

The middle terms are known during the time-stepping of the model. If the neutral value for C_N (i.e. the standard value that ignores the stability effects in J.-F. Louis' formulas), the anemometer speed v_{an} turns out to have the desired daytime maximum and nighttime minimum. (These values are being examined by the Techniques Development Laboratory as a possible input to the MOS equations for surface wind, but the values are not otherwise transmitted anywhere.)

2. Mixing of heat and moisture in the bottom layers of the NGM.

Except for the process of cumulus convection, turbulent vertical diffusion of heat and moisture occurs only in the bottom layers of the NGM, and only through the special boundary layer mixing model described in this section.

The calculation is based on the ideas first proposed by Ball (1960), as modified and used by Lilly (1968), Deardorff(1985), Driedonks(1981) and others. Ball introduced the important consideration that turbulent mixing, if it is to be important, must be intense enough that the turbulent kinetic energy is almost in a steady state, so that the processes acting to create it and to destroy it must add up (approximately) to zero. In a closed volume, these processes are

(a) creation by buoyancy effects when the air is cooler than the ground,
(b) creation by the mechanical effect of air flow over rough ground,
(c) dissipation by molecular viscosity

It can be shown by order-of-magnitude arguments that (c) is small in comparison to either (a) or (b), whenever those processes are significant.

As an example consider the effect of surface heating in the morning as it changes the stable lapse rate that existed at sunrise, in a condition where the ambient wind is weak enough that the mechanical process (b) can be ignored. Older arguments would simply take the energy available from the hot surface (i.e. the turbulent heat flux) and construct the new lapse rate as that adiabatic line

whose intersection with the original temperature curve would enclose an area corresponding to the energy represented by the heat flux. This calculation is indicated on Figure 3.

Observation shows that this is not what occurs (Figure 4.) The observations are consistent with the conclusion that process (a) must be close to zero-- the decrease in potential energy represented by the warming in the bottom layers is balanced by the increase in potential energy represented by the cooling of the layers higher up. Evidently the turbulent eddies caused by the surface heating are intense enough to mix the air above the mixed layer with the air in the mixed layer. This process whereby quiescent non-turbulent air is mixed into adjacent turbulent air is called "entrainment".

Numerical details of these calculations for the NGM are given in NMC Office Note 318, April 1986. A simplified presentation is as follows.

$$b = \text{"buoyancy"} = g \times \text{virtual potential temperature} \approx C_1 \times \theta + C_2 \times q \tag{6}$$

$$\frac{\partial}{\partial t}\int \rho\, b\, dz = \text{buoyancy flux from ground} = C_3 \times \text{Heat Flux} + C_4 \times \text{Evaporation} = B \text{ , say.} \tag{7}$$

$$\frac{\partial}{\partial t}\left[\text{Potential Energy}\right] = -\int \rho\, b\, z\, dz = -0.4\ \text{"h"}\ B + 2.5\ \rho_o\, u_*^3 \tag{8}$$

[Conversion to kinetic energy] [Energy added by mechanical stirring]

"h" is the "depth of the mixed layer". The factor 0.4 was measured by Deardorff in laboratory experiments. (It is less than 0.5 because the mixing just above the mixed layer corresponds to a downward flux of heat.) The last term on the right represents a lifting of the center of mass of the column by mixing from eddies arising from flow over rough terrain. The factor 2.5 corresponds to the experience of Driedonks in the field experiment analysed by him. u_* is the friction velocity.

This physical reasoning results in integral statements about a column in the bottom part of the atmosphere. In all previous applications of these concepts, however, in oceanography and meteorology, the mixed depth "h" was introduced as a new model variable. In numerical models, this has caused considerable problems, in addition to having to decide what to do about "h" after sundown! In the NGM,

these integrals are applied directly to the bottom layers of the model.

This has eliminated all numerical problems.

The stirred layers have a uniform θ and a uniform q. The length "h" in (2) is not a new forecast variable, but is interpreted as the depth of the number of layers that at any moment have already been mixed for each separate grid column.

The mechanical stirring effect can be significant over land in winter when the surface buoyancy flux (B) is small and winds are strong . In summer, the mixed layers can extend up to 700 mbs in the southwestern part of the United States.

The advantages of this parameterization seem to be as follows.

a. It is based on laboratory (Kato,Deardorff) and field (Miyake,Driedonks) experiments.
b. In contrast to other formulations of the Ball model, there is no problem with "h" at night time, and there seem to be no problems associated with geostrophic balance at the top of the mixed region.
c. In single column computations, the results match closely those obtained for an explicit "h" model.

Weaknesses are as follows.

a. At present the code does not recognize the effect of saturation on buoyancy.
b. Momentum exchange is treated separately, and the effect of shear at the top of the mixed layer in enhancing mixing is ignored.

Problems: No major problems have been identified as yet. Accumulation of too much q at the top of the mixed layers has not as yet been a problem in 48-hour forecasts, even though this process and the Kuo convective precipitation adjustment are the only methods for turbulent mixing of moisture in the vertical. (There is no vertical austausch mixing of moisture or entropy.)

3. Results of low-level cool-season temperature forecasts.

The bottom layer of the NGM is about 35 millibars thick, so that variables in the middle of this layer are located about 150 meters above the ground surface in the model.

OBSERVED AND COMPUTED VARIANCES

The top diagram of Figure 5 shows the standard deviation of the temperature at this level as computed from the zero-hour forecasts from 58 NGM forecast runs, both 00 and 12GCT, beginning with that of 00GCT, 21 January 1988. The bottom diagram shows the same field computed instead from the 48-hour forecasts of these same 58 forecast runs. Since both 00GCT and 12GCT cycles are included, these variance fields contain effects from both the diurnal cycle and synoptic events. The similarity between the 0-hr and the 48-hr forecast fields is striking, and many of the differences probably have good explanations. For example, the forecast values at 48 hours east of the Gulf Stream are one or two degrees larger than those at 0 hours. This suggests that heat flux into the atmosphere from the ocean may be underestimated in the NGM, so that the temperature in the bottom layer does not accomodate quickly enough to the relatively fixed field of ocean surface temperature.

VARIANCE OF FORECAST ERRORS

Figure 6 shows the standard deviation of the forecast errors at 24 hours and at 48 hours, the errors being defined by comparison with the verifying 0-hour output. Forecasts from both 00 and 12GCT are included.

The forecast errors are generally less than the "observed" variance on Figure 5 , with a few exceptions. One of these is over water, near Juneau. In such a location, the NGM temperature forecast has more error than would a persistence forecast.

Comparison with Figure 5 shows that the two areas of maximum error-just east of the Divide and around West Virginia---are in areas of high variability of temperature at this level.

The 24-hour and 48-hour values are almost equal in the western third of the continent, i.e., in the mountains. In such regions, the explanation of these "errors" must include either random errors in the verifying 0-hour fields, or a basic mismatch between model and analysis system, with respect to how the analysis system assigns the initial temperature values for the model.

THE DIURNAL CYCLE

Something approaching the diurnal cycle can be obtained by comparing fields of temperature in the bottom layer at 00GCT (1800 local time in the Midwest) with those at 12GCT (0600 local time in the Midwest). Figure 7 shows the average difference 00GCT minus 12GCT for 28 days beginning with January 21 1988. The top diagram shows this difference as given by the 0-hour output from these days, while the bottom diagram shows the forecast value of this difference at 48 hours from the same 56 forecast runs. The overall agreement between these two maps over land is reasonable. Some aspects of the 48-hour field seem "better" than the zero-hour field, such as the more reasonable (higher) values in Western Colorado and Utah. The 0-hour output seems better in other details, such as the lack of a center in Southwestern Alaska. No explanation is at hand for the tendency at 48 hours for small negative values close to the coasts over water, although a continental diurnal circulation may be suspected.

MEAN ERRORS

Figure 8 shows the 48-hour mean errors that accompany the standard deviation of the errors shown in Figure 6 . (Forecasts from both 00 and 12GCT are included.) The tendency toward a positive error in the eastern and a negative error in the western half of the United States shows up here.

The concentration of the positive error along the axis N. Dakota - Texas suggests that there is too much downslope motion in the model east of the continental divide. (The alternate possibility, that the analysis produces consistently an analysis that is several degrees too cold, does not seem likely, since the model terrain is higher than the actual terrain in this region, so that surface inversions in the radiosondes are probably ignored rather than overemphasized.)

c. Much of the pattern present in Figure 8 is present in other months, especially the negative values in the West. Figure 9, for example, contains the same 48-hour mean "errors" in T of the bottom layer for 62 forecasts in March 1988. The many centers of negative errors are present on both charts, the only exceptions being the lack in March of a center near Juneau and in Michigan.*

* The presence or absence in the NGM of ice on the Great Lakes has not been resolved satisfactorily as yet. The same uncertainty exists in the global data assimilation system that provides the first guess for the RAFS analysis. It may not be irrelevant that this negative center in Michigan is centered between radiosonde locations.

Three positive centers (northwestern Canada, eastern Canada, bottom of the Baja peninsula) are repeated, but the Texas -North Dakota center of January-February appears further eastward in March, on the Iowa-Illinois border.

d. Some further idea of the fixed nature of the mean "errors" in T of the bottom layer can be seen in Figure 10, which shows the 12-hour "errors" for the same forecasts whose 48-hour errors were shown in Figure 8. Most of the centers have a magnitude at 12 hours that is much more than 1/4-th of their magnitude at 48 hours, indicating that whatever mismatch exists between the climatology of the zero-hour fields and the climatology of the model is rapidly resolved by the model.

e. Temperatures from the 50-mb thick "boundary layer" of the LFM are not archived, but the potential temperature of this layer is archived. Figure 11 contains the mean 48-hour error for this field (verification being against the LFM 0-hour output), for 60 forecasts made in March 1988. The oceanic values are clearly too large, undoubtedly because the LFM incorporates turbulent heat transfer from ocean into this layer, but has no mechanism for turbulent transfer upwards out of this layer. From the present perspective, however, the most interesting feature of this Figure is the string of negative centers located approximately along the Continental Divide, and the center near Yosemite, since these features are also present in the NGM results.

f. An interesting correlation with the negative centers on Figures 8-11 appears in Figure 12, which shows the difference in height between the enhanced orography used in the T80 global models at NMC (including the Global Data Assimilation System) and the NGM. The main source of this difference is the artificial enhancement used for the global models, since the NGM orography is based on a T72 spherical filter.*

*A two-week comparison test in which the global assimilation system used T80 "mean" orography (i.e. without the artificial enhancement that is used operationally) was conducted in January 1988, and parallel analyses and forecasts were made with the Regional system from this first guess. Unfortunately the writer's attention for this test was focussed on possible changes in the NGM forecasts of 500-mb height and tropospheric thickness values, and he neglected to examine possible changes in the 0-hour temperature of the bottom layer until the parallel archive for this test had been written over. Mea culpa.

Further effort on diagnosing and solving this problem--such as examining the low-level temperature error field in the Aviation Model-- is warranted.

4. Lapse rate effects in the case of 00GCT January 12 1988.

This case was an example of a cold air outbreak that was not exceptionally extreme. It was forecast reasonable well by the operational NGM, as shown by the synoptic charts on Figures 13 and 14.

Figures 15, 16, and 17 show temperature profiles from the bottom 8 levels of the model, at three sites in the region invaded by the cold air. In addition to the initial profiles for 00GCT on the 12th and 00GCT on the 14th, two predicted profiles are shown, one for the operational forecast, and one for a forecast in which radiation was turned as well as the vertical mixing of moisture and heat. The latter curves (dashed) show the typical error present in the NGM temperature forecasts prior to the addition of physics to the model in 1986---the bottom temperature is too cold and the lapse rate in the bottom levels is much too stable. This spreading of cold air is associated with the baroclinic processes that are present in the real atmosphere and in the model.

The dotted curves in the Figures are the results of the complete operational forecast model. They show how the baroclinic spreading of cold air in the model has now been balanced to a considerable extent with the natural processes of heat exchange by radiation and low-level turbulence.

REFERENCES

Ball. F., 1960: Control of inversion height by surface heating. Q. J. Royal Meteor. Soc., 86,483-494.

Deardorff, J. and G. Willis, 1985: Further results from a laboratory model of the convective planetary boundary layer. Boundary Layer Meteorology,32, 205-236.

Denman, K., and M. Miyake, 1973: Upper layer modification at Ocean Station PAPA: observations and simulation. J. Phys. Ocean., 3, 185-196.

Driedonks, A., 1981: Dynamics of the well-mixed atmospheric boundary layer. Scientific Report W.R. 81-2, Konin. Neder. Meteor. Inst., De Bilt, 189 pp.

Izumi, Y., 1964: The evolution of temperature and velocity profiles during breakdown of a nocturnal inversion and a low-level jet. J. Applied Meteor.,7,78-79.

Lilly, D., 1968: Models of cloud-topped mixed layers under a strong inversion. Q. J. Royal Meteor. Soc., 94, 292-309.

Louis, J-F, 1979: A parametric model of vertical eddy fluxes in the atmosphere. Boundary Layer Meteorology, 17, 187-202

National Weather Service, 1986: Modeling of physical processes in Nested Grid Model. Technical Procedures Bulletin 363. Silver Spring, Md. 24 pages.

Phillips, N., 1986: Turbulent mixing near the ground for the Nested Grid Model. Office Note 318, National Meteorological Center, National Weather Service(NOAA) 19 pp.

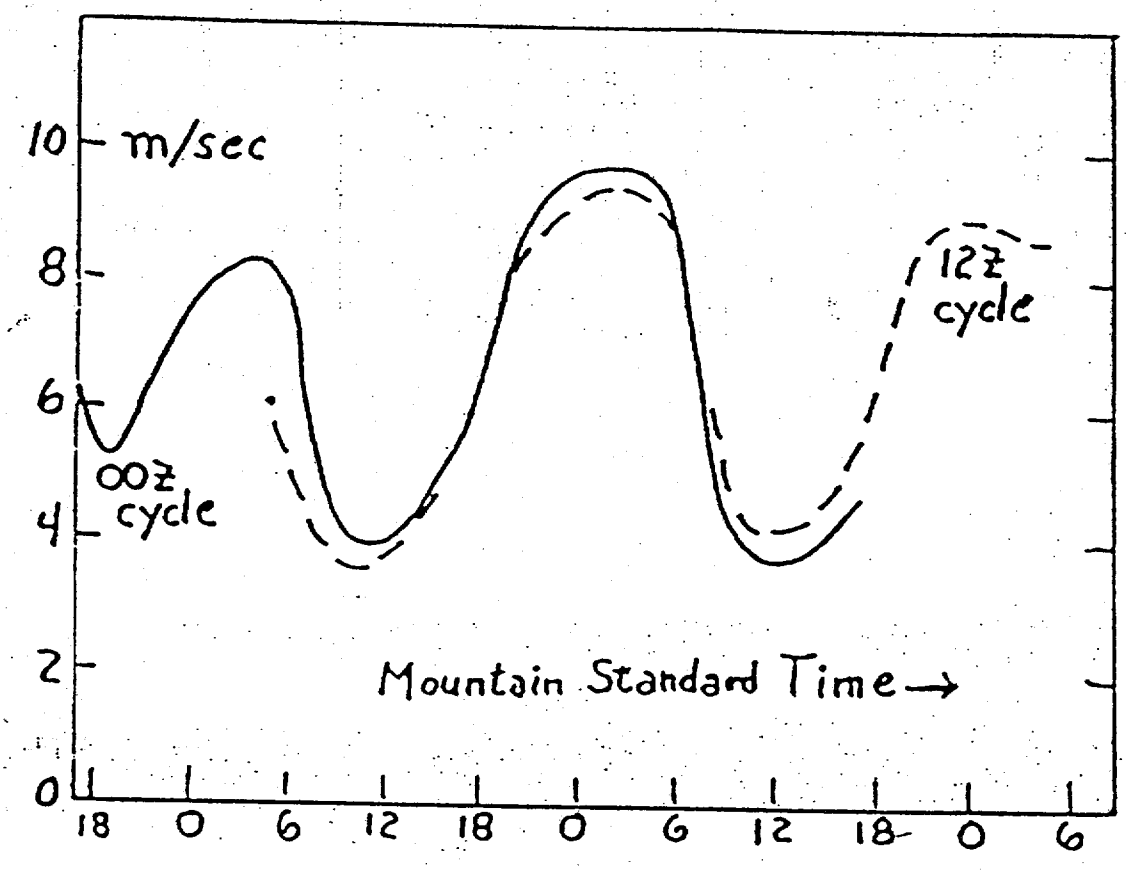

Fig. 1. The diurnal variation of wind speed in layer 1 forecasts, shown separately for 22 forecasts from 0GCT and from 12GCT, made in June 1986, and averaged over four locations in eastern Colorado.

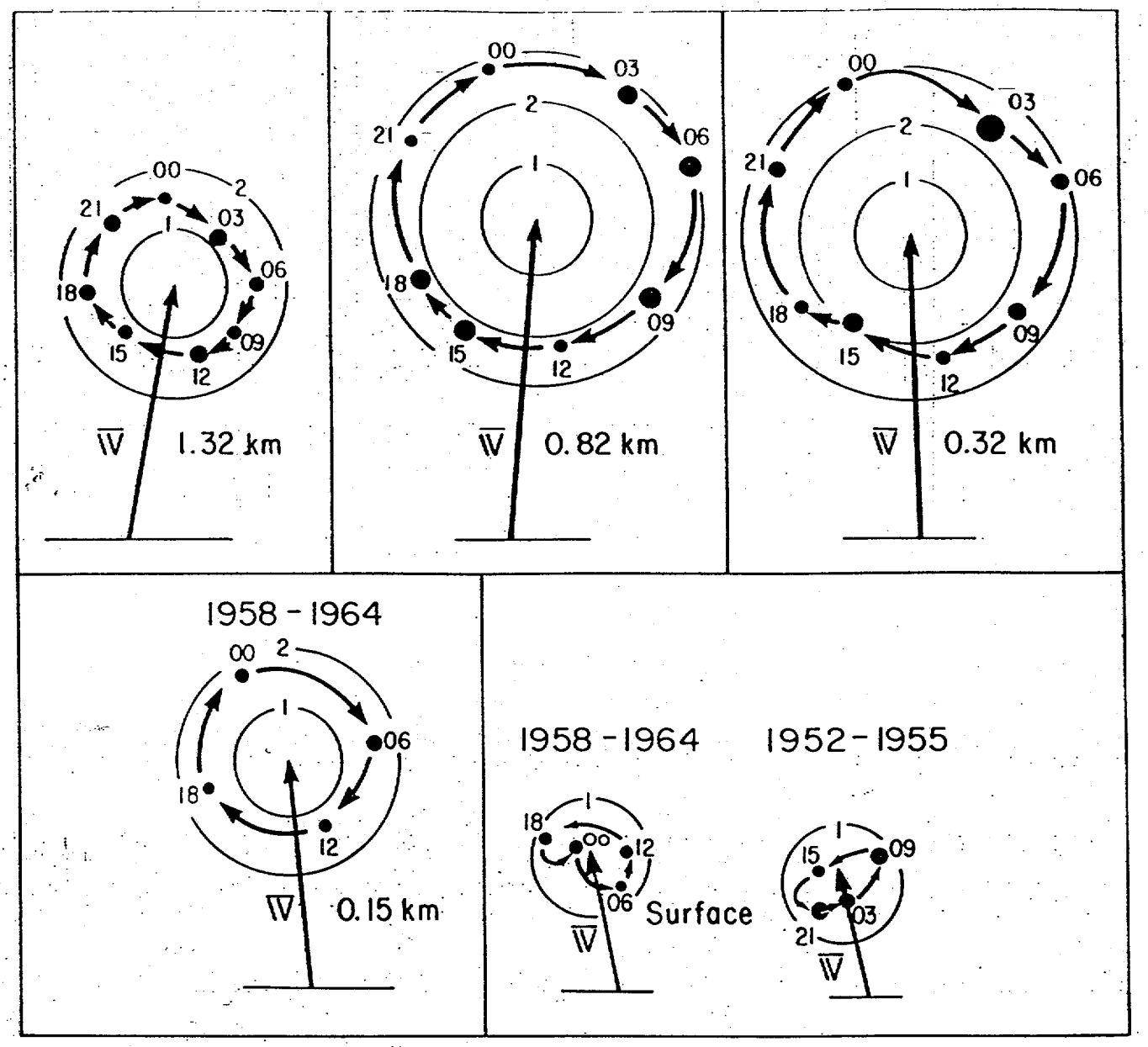

Fig. 2. Diurnal velocity hodographs at several levels from data measured in the South-Central United States in summer. From Bonner and Paegle (1970). The radius of the velocity circles appears to be about 2 to 3 m/sec. Times (Central Standard) in hours are plotted for each point on the graphs.

F2

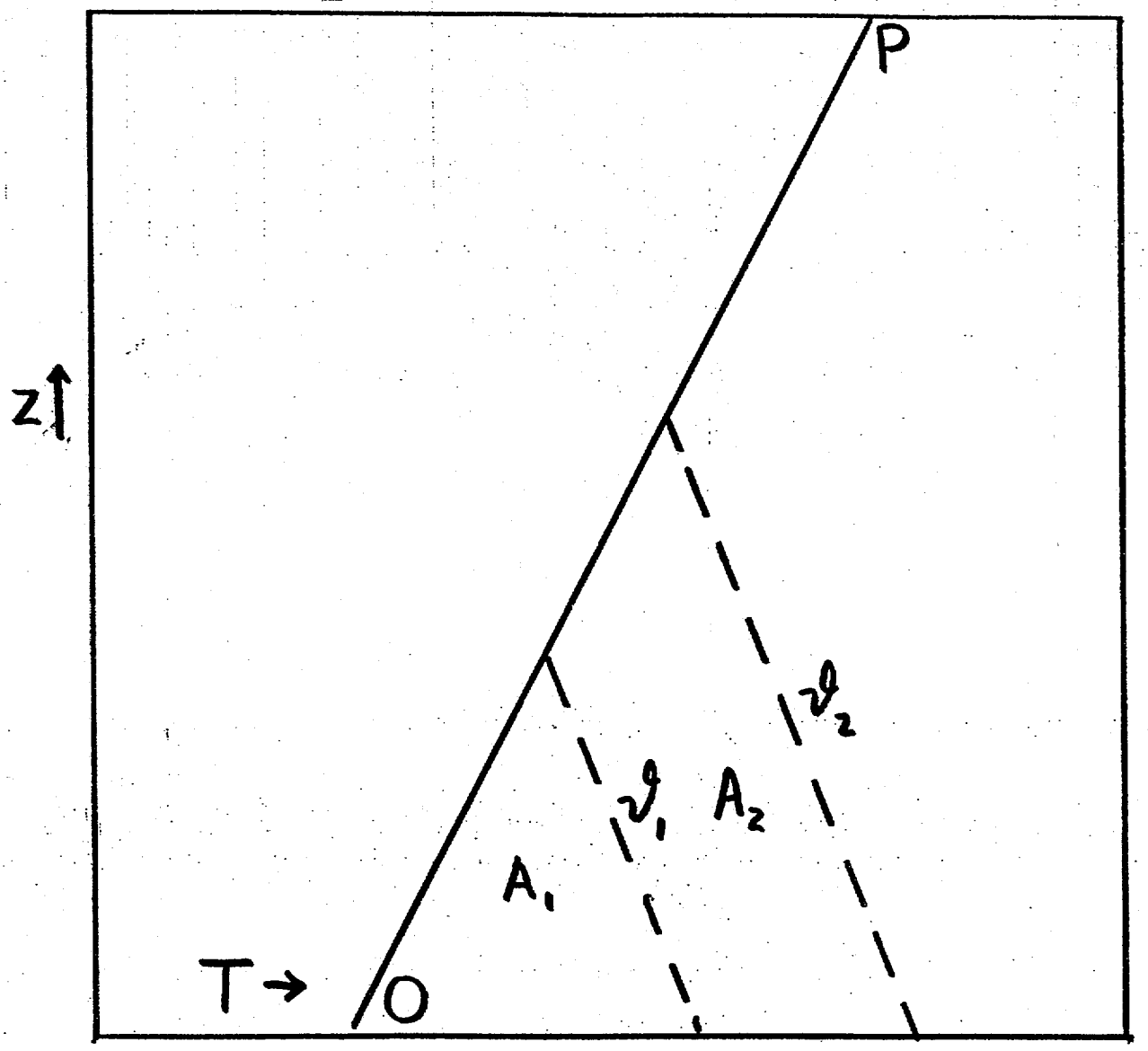

Fig. 3. Schematic sketch of the classical manner of estimating the change to a stable lapse rate caused by heat transfer from the underlying surface. The original temperature profile is indicated by the line OP. θ_1 and θ_2 are adiabatic lines, so chosen that area A_1 corresponds in energy to the sensible heat created by time t_1, and area A_2 corresponds to the energy added between times t_1 and t_2 .

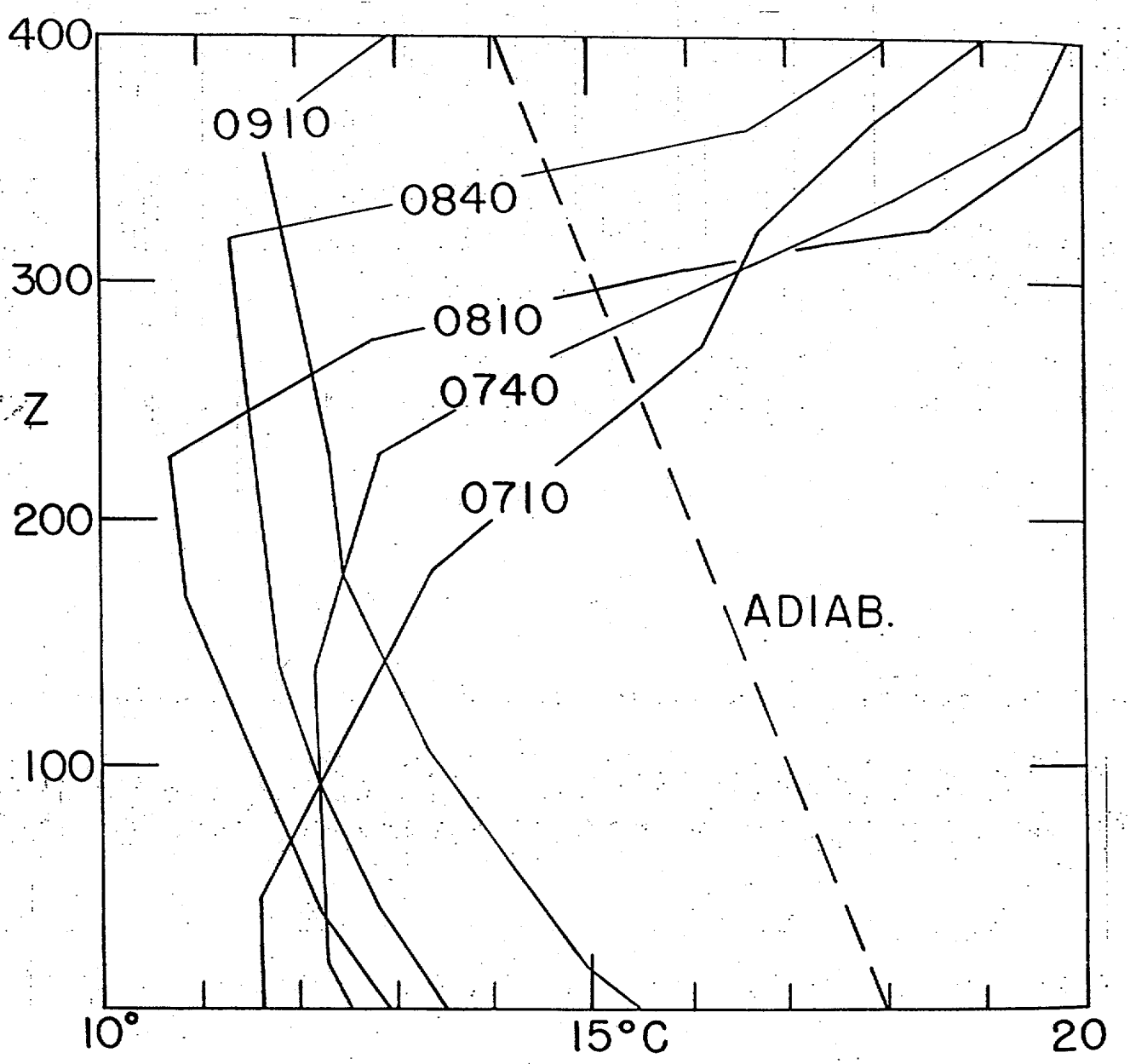

Fig. 4 Observed temperatures on a clear morning in Texas (local time). The dashed line is an adiabat. Measurements were made at only 12 heights; kinks in the profile may be due to this. (Adapted from Y. Izumi, J. Applied Meteorol., 3, 1964, p. 73.)

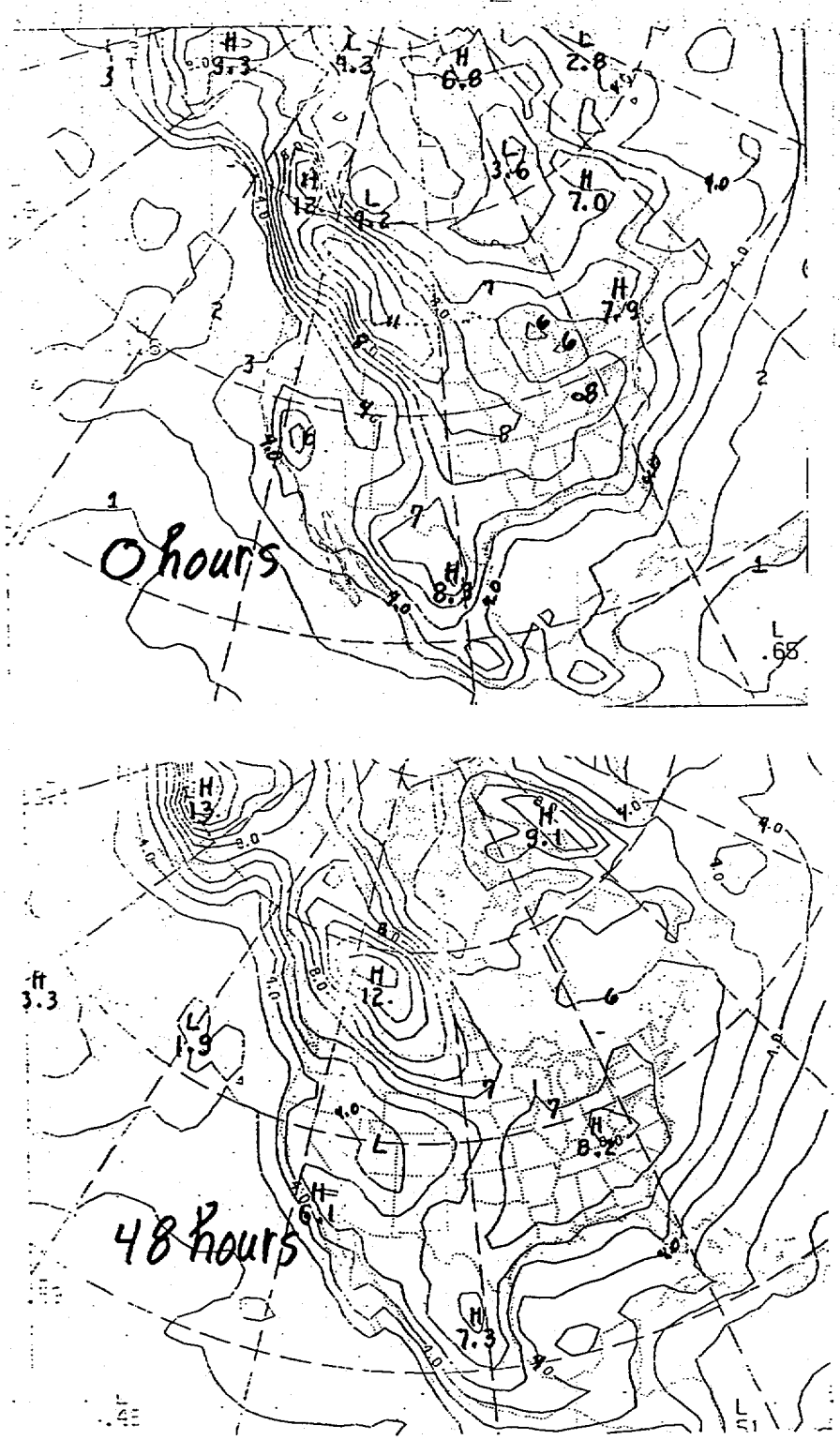

Fig. 5. Standard deviation of the temperature in the bottom layer over 58 consecutive forecasts beginning at 0GCT, 1/21/88. Values are computed from 0-hour outputs and (separately) from 48-hour outputs. Isolines are at intervals of one degree.

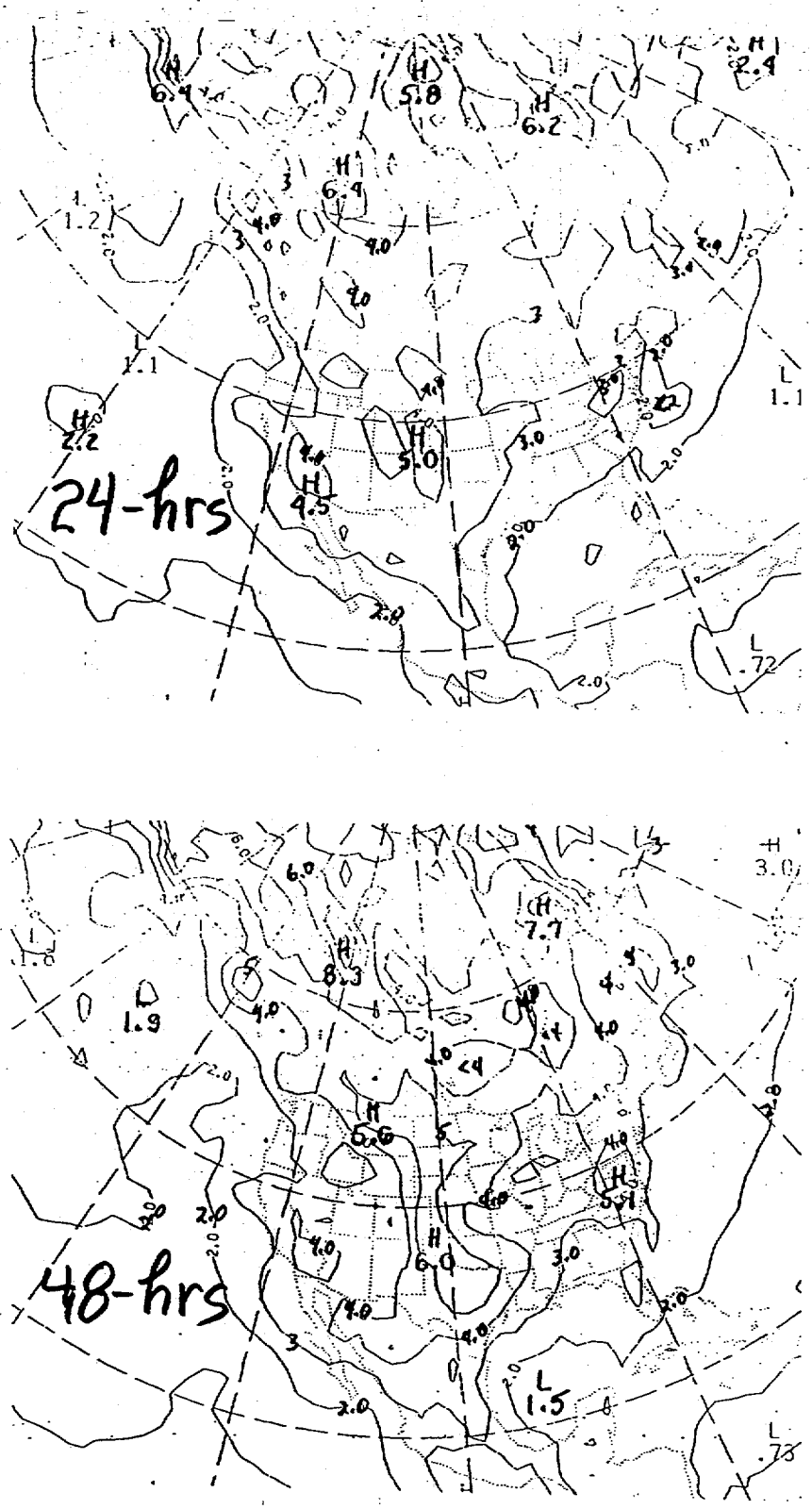

Fig. 6. Standard deviation of the 24- and 48-hour forecast errors for temperature in the bottom layer, computed from 52 consecutive forecasts beginning with OGCY, 1/20/88. Isolines are at intervals of one degree.

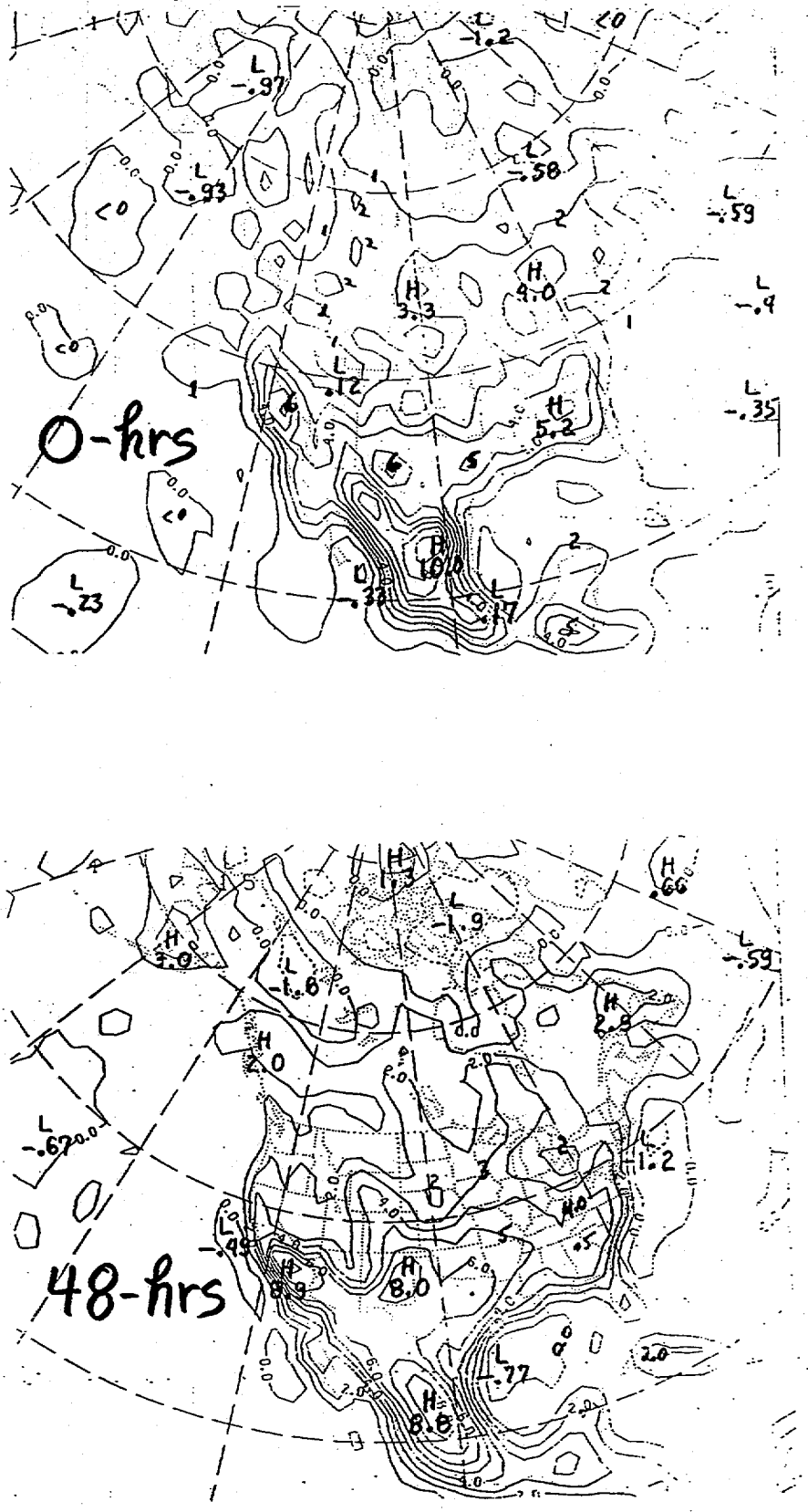

Fig. 7. Average differences between 0GCT and the following 12GCT values of temperature in the bottom layer, averaged over 30 successive days beginning with 1/21/88. Values are shown separately for the 0-hour and the 48-hour fields. Isolines are at intervals of one degree.

F7

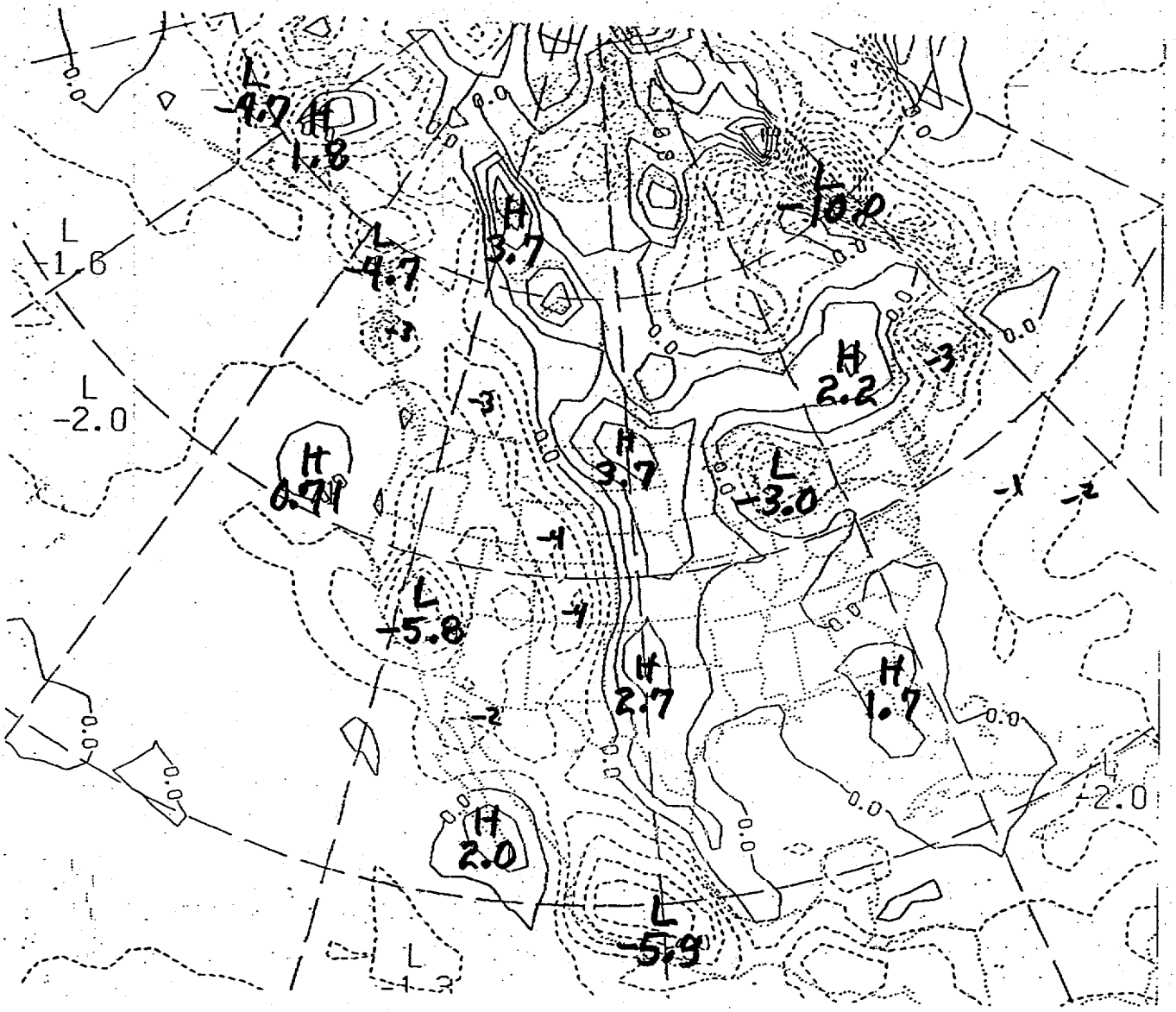

Fig. 8. Mean error in 48-hour forecasts for temperature in the bottom layer, calculated from a series of 50 consecutive forecasts beginning with 0GCT, 1/20/88. The verifying field was the 0-hour output at the verifying time. Isolines are at intervals of one degree, with negative values dashed.

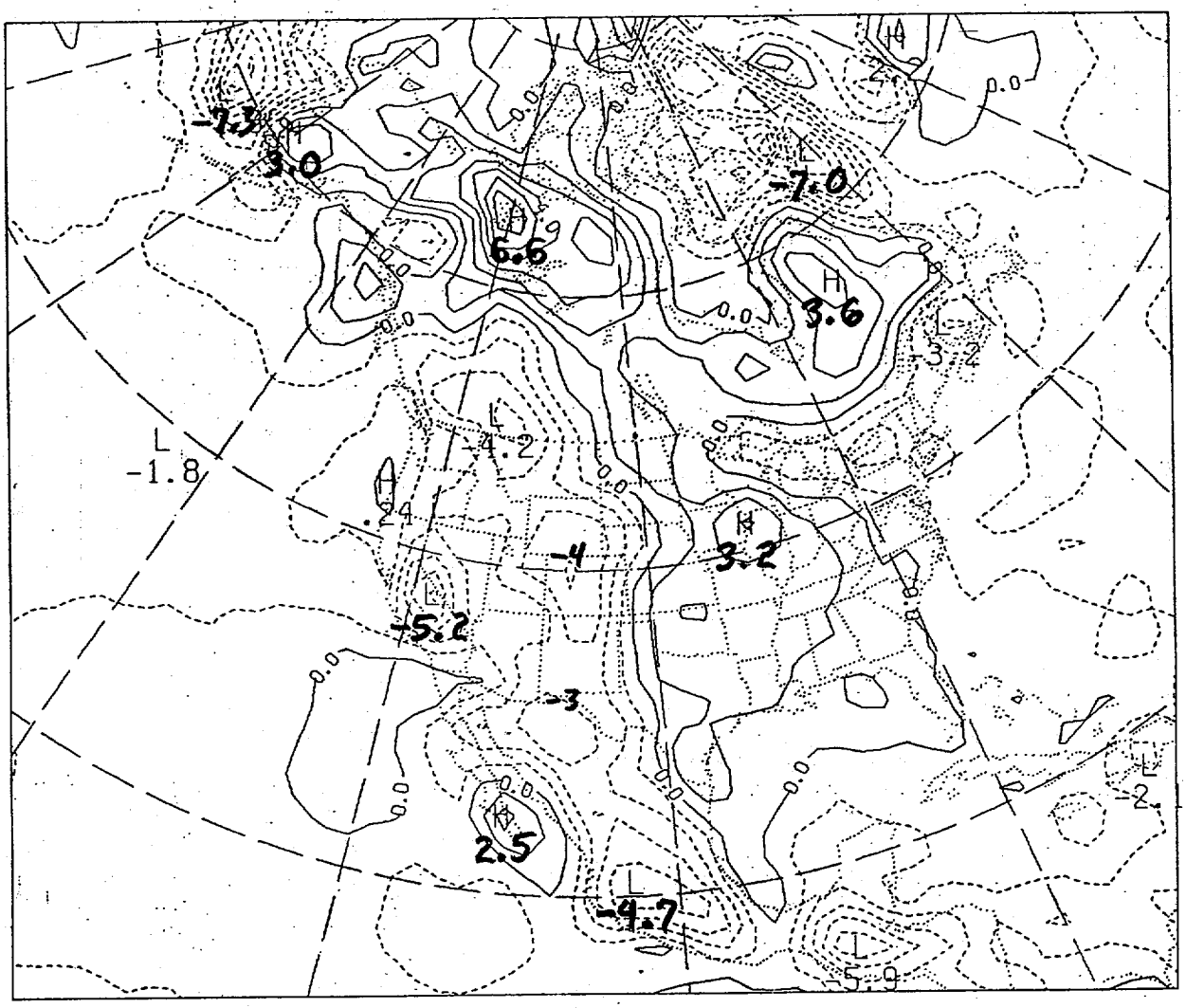

Fig. 9. Same as Fig. 8, but for the 62 NGM forecasts beginning with 00GCT on March 1 1988.

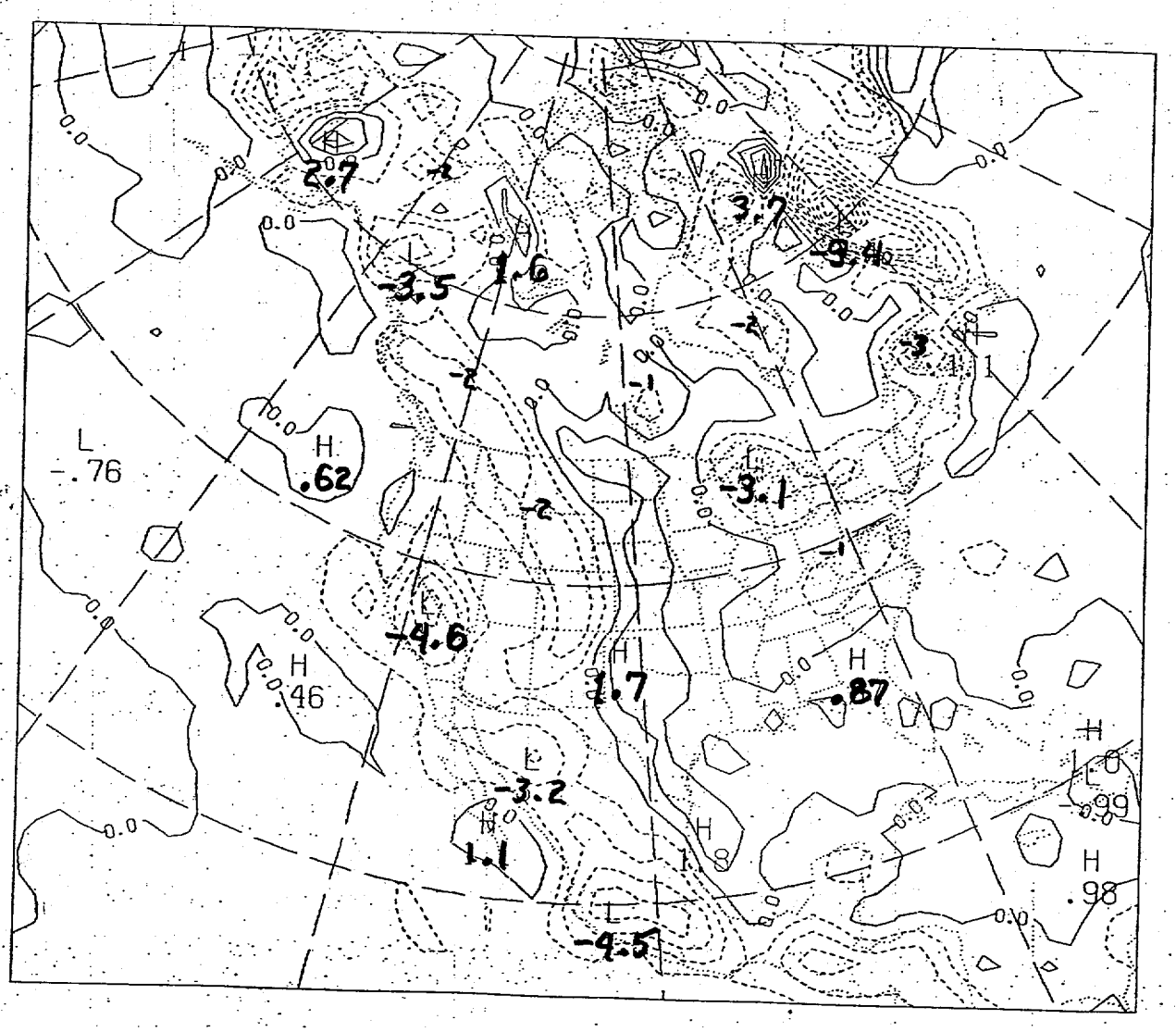

Fig. 10. Same as Fig. 8, but for the corresponding 12-hour forecasts.

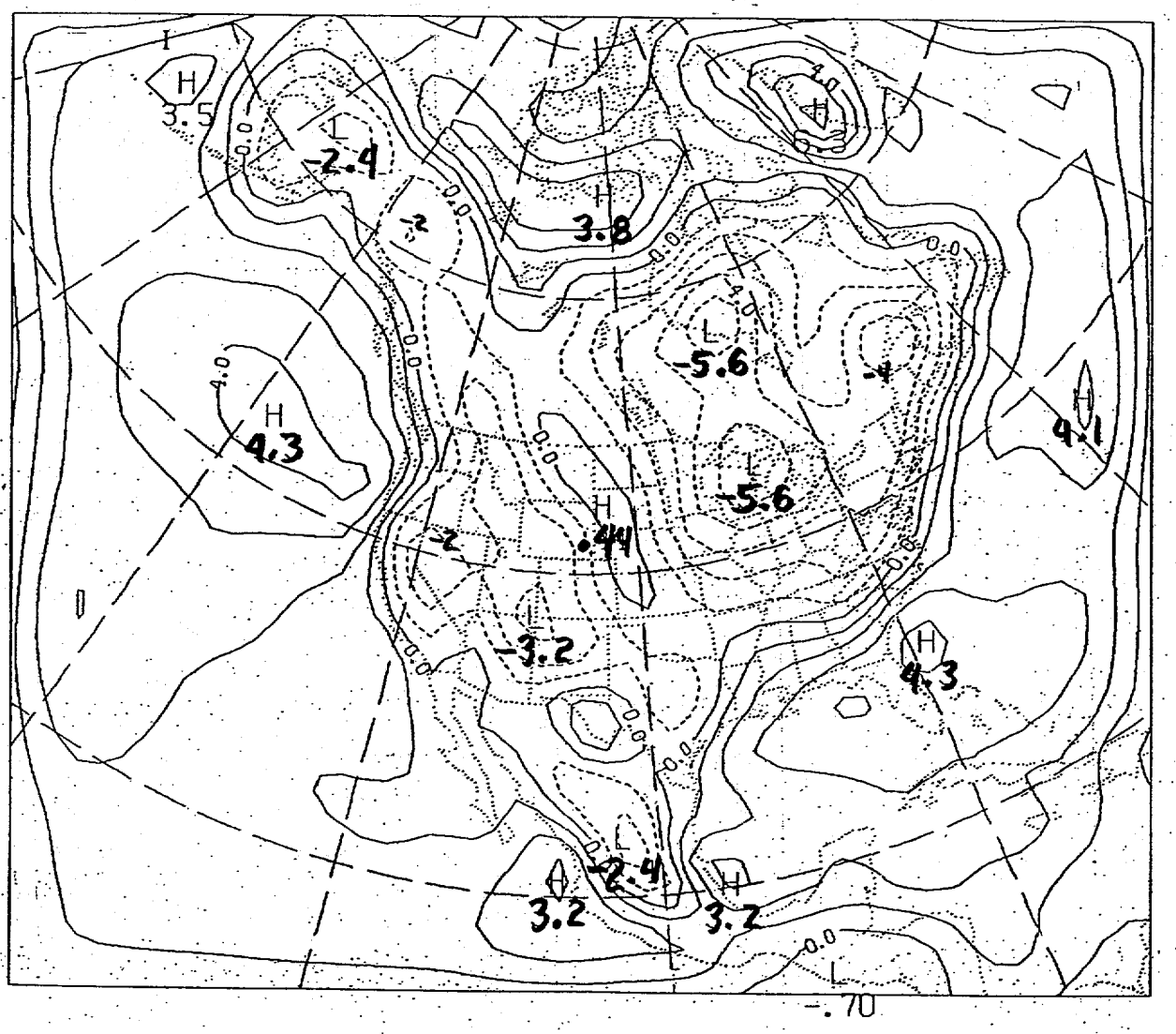

Fig. 11. Mean 48-hour error in the potential temperature of the boundary layer in the Limited area Fine Mesh (LFM) model for 60 forecasts in March 1988.

F10

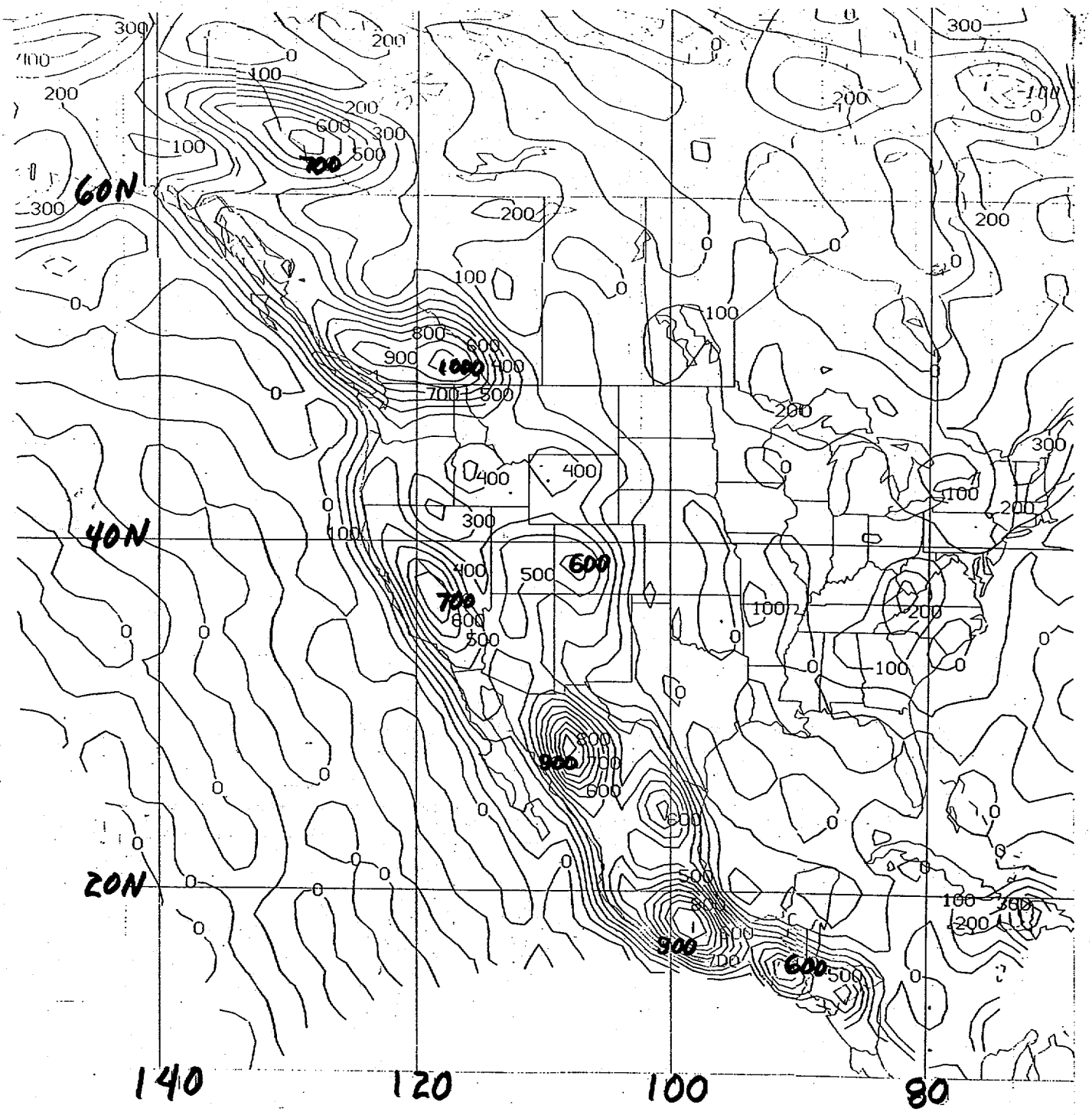

Fig. 12. Difference in ground elevation between the enhanced orography used in the T80 global models at NMC and the unenhanced orography used in the NGM. Units are meters. Positive values mean that the global orography is higher.

F12

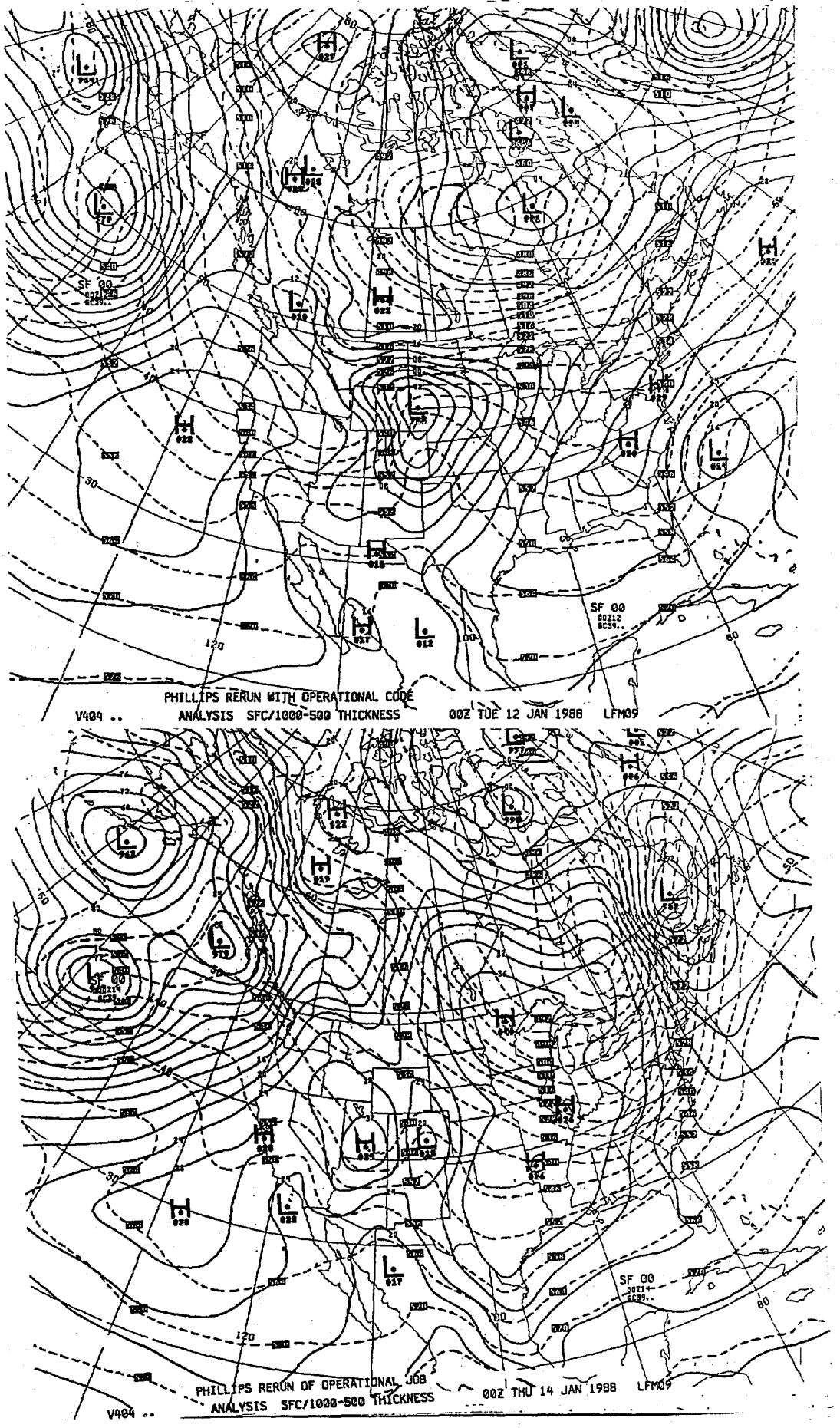

Fig. 13. Top: Initial analysis for 00GCT 12 January 1988. Bottom: Verifying analysis for 00GCT 14 January 1988.

F13

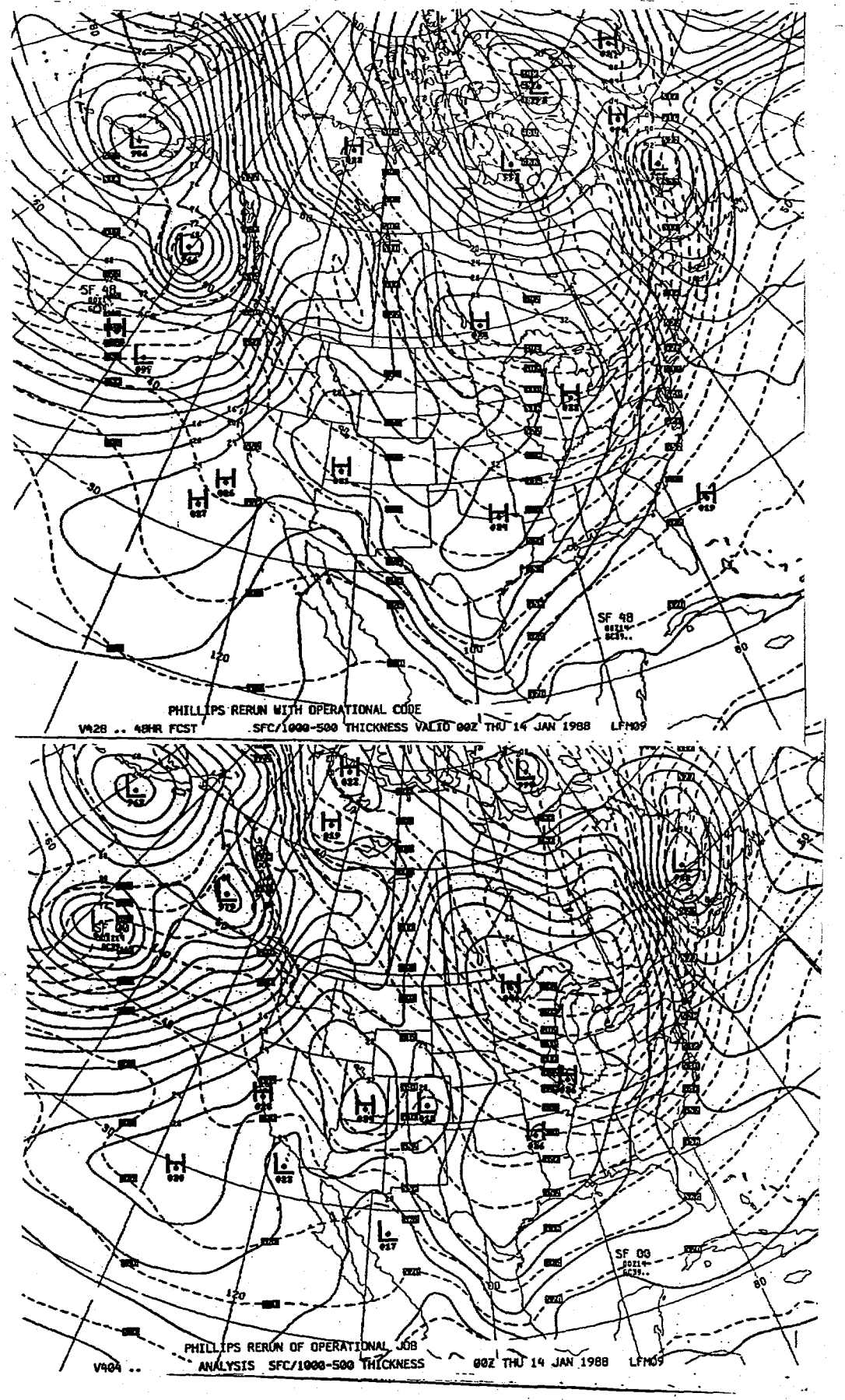

Fig. 14. Top: 48-hour forecast from 00GCT 12 January . Bottom: Verifying analysis for 00GCT 14 January 1988 (a repeat of the bottom of Figure 13).

F14

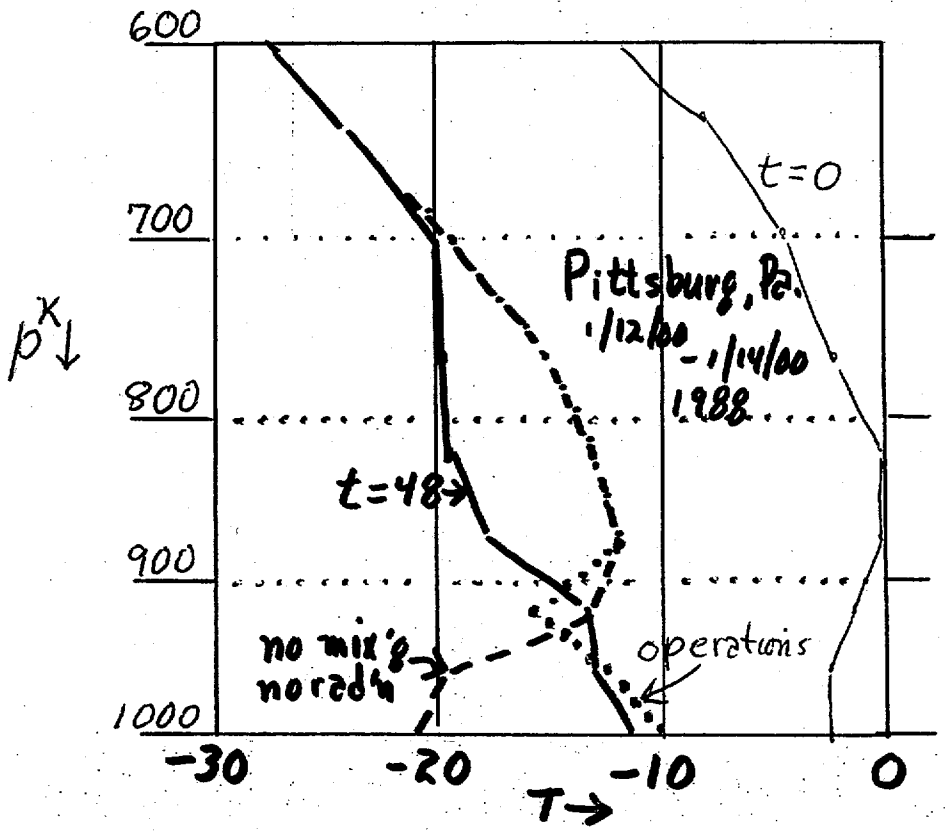

Fig. 15. NGM profiles of temperature for the bottom 8 levels in the model at Pittsburg, Pennsylvania

Thin solid: Initial profile for 00GCT 12 January 1988
Heavy solid: Initial profile for 00GCT 14 January 1988
Dotted: Operational 48-hour forecast from 00GCT 12 January
Dashed: Forecast with no mixing of heat and moisture and no radiation

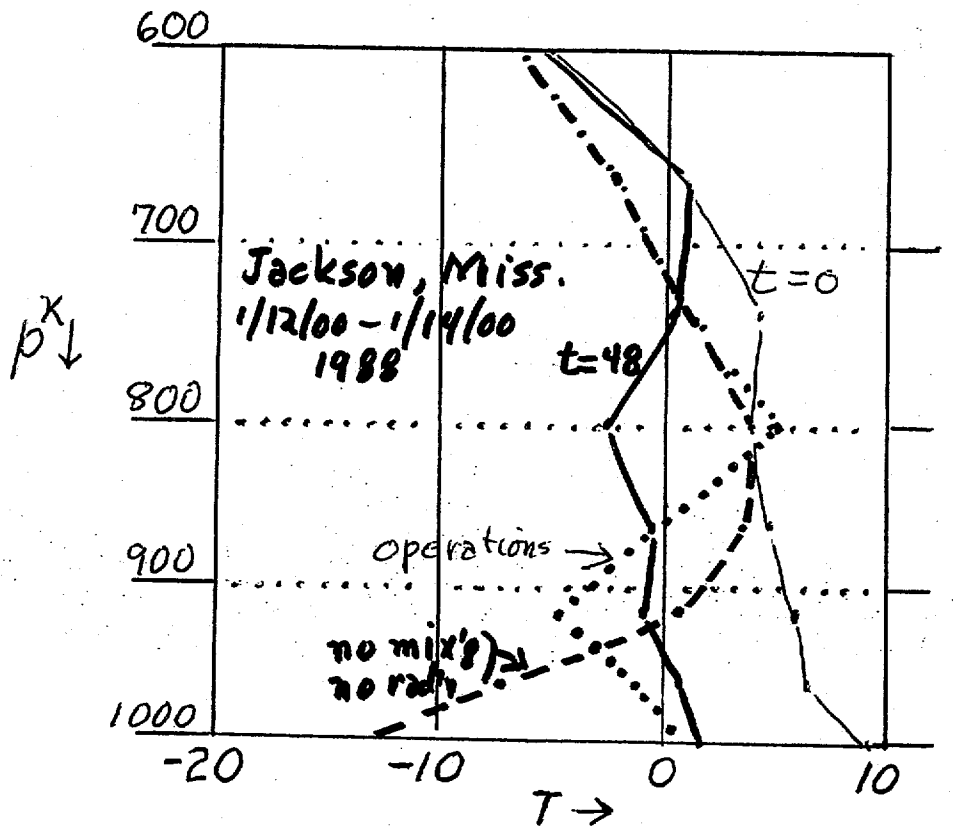

Fig. 16. As for Figure 15, but for Jackson, Mississippi.

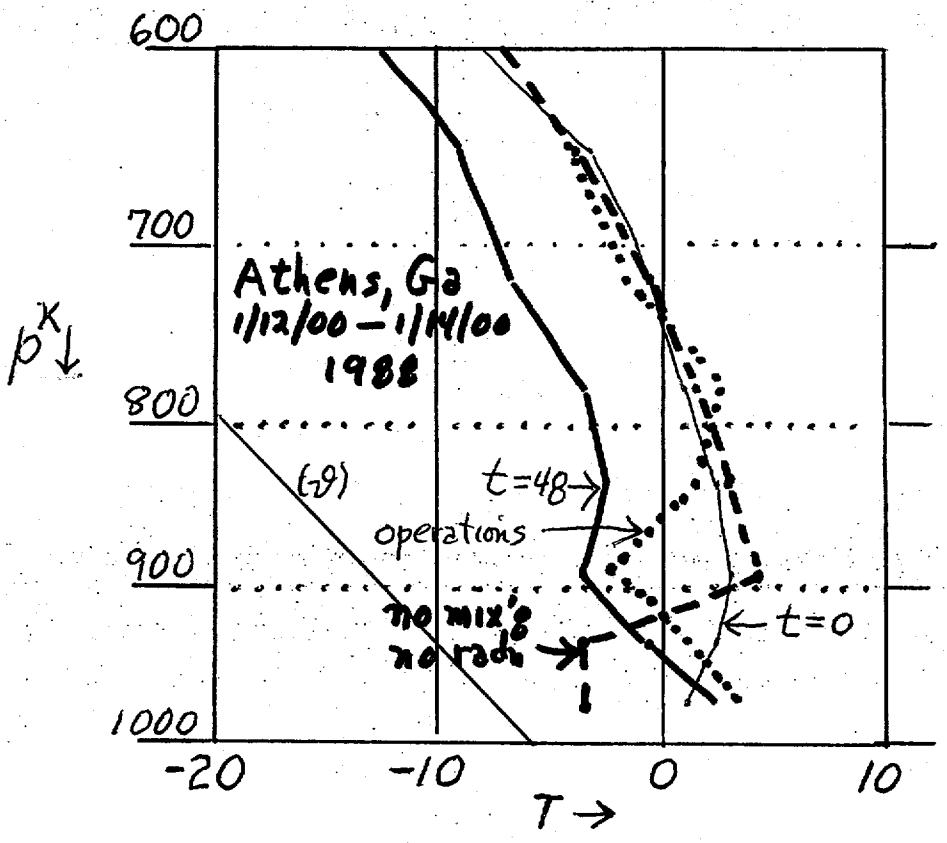

Fig. 17. As for Figure 16, but for Athens, Georgia.

F17